[12]H. R. Child, W. C. Koehler, and A. H. Millhouse, J. Appl. Phys. 39, 1329 (1968). These authors report neutron-diffraction results for rare-earth–thorium alloys which are interpreted in terms of short-range antiferromagnetic correlations. We are currently studying this more completely.

ELECTRONIC STRUCTURE OF THORIUM METAL. II. THE de HAAS–van ALPHEN EFFECT*

D. J. Boyle† and A. V. Gold‡
Institute for Atomic Research and Department of Physics, Iowa State University, Ames, Iowa 50010
(Received 9 January 1969)

High-resolution studies of the de Haas–van Alphen effect in thorium, although not yet complete, are found to provide strong support for the validity of a new model for the Fermi surface proposed by Gupta and Loucks in a companion paper.

Thorium is thus far the only metal in the actinide series for which experimental data exist relating to the details of the electronic structure and the Fermi surface. A de Haas–van Alphen (dHvA) effect in thorium was first observed by Thorsen, Joseph, and Valby[1] about two years ago, but these authors experienced considerable difficulty in resolving the various dHvA frequency branches in their impulsive-field experiments. At that time, the crystals available were of relatively poor quality, with resistivity ratios $R_{293°\mathrm{K}}/R_{4.2°\mathrm{K}}$ less than 100; and techniques for the digital recording and analysis of impulsive-field dHvA data had not been developed. In consequence, Thorsen, Joseph, and Valby were not able to claim a unique interpretation of many of their results. The availability of thorium samples of somewhat higher quality at this laboratory[2] and the current interest in first-principles calculations of the band structure of the actinides[3] have motivated us to reexamine the dHvA effect in thorium.

Our samples were prepared from thorium refined by means of the electrotransport method.[4] $R_{293°\mathrm{K}}/R_{4.2°\mathrm{K}}$ for a strain-annealed rod from which the crystals were cut was approximately 160 (a disappointingly low figure considering the fact that ratios as high as 1200 have been reported for polycrystalline thorium refined by the same technique).[5] Our crystals were roughly cylindrical in shape with typical dimensions about 1 mm. The samples were studied in a 61-kG superconducting solenoid, the field strength being monitored by the NMR of an Al^{27} specimen in the immediate vicinity of the thorium crystal.[6] The signals were detected inductively through parallel modulation of the main field H by an alternating field of frequency $\nu \sim 40$ Hz and amplitude $\lesssim 150$ G, which could be programmed to vary as H^2. Stark's over-modulation technique[7] was used throughout, with the lock-in amplifier usually tuned to either 2ν or 4ν. The data were recorded digitally, and then analyzed by the filter-periodogram method.[8]

As was also found by Thorsen, Joseph, and Valby,[1] our dHvA frequencies were observed to fall, broadly speaking, into two distinct sets (see Fig. 1); in addition, a new low-frequency branch A was detected. The oscillations in the 11- to 14-MG range are fairly complex, and the important feature of this work is that we have been able to resolve these data into distinct frequency branches. The smooth curves superimposed on the experimental points in Fig. 1 are the frequency variations expected from the Fermi surface predicted by Gupta and Loucks,[3] with the small letters referring to the extremal orbits shown in Fig. 2; the areas $\mathcal{A}$ of these orbits have been translated into dHvA frequencies using the Onsager relation $F = (\hbar c/2\pi e)\mathcal{A}$. The Gupta-Loucks model actually gives rise to more frequency branches than we have been able to detect thus far, and for the sake of clarity we have used solid curves in Fig. 1 to indicate those portions of the model branches which are considered to correspond to the available data; the predicted frequency variations are shown as dotted curves elsewhere.

The experimental and theoretical curves which are believed to be related to one another have been labeled with the same letters, capital and lower case, respectively, and these relationships have been established in a fairly unambiguous fashion from symmetry considerations. Thus, beginning with the frequencies around 12 MG, we note for example that the symmetries of the observed branches in the vicinity of the ⟨100⟩ frequency M have an immediate counterpart in the predicted frequency variations for extremal orbits of type m. Likewise, the observed crossing

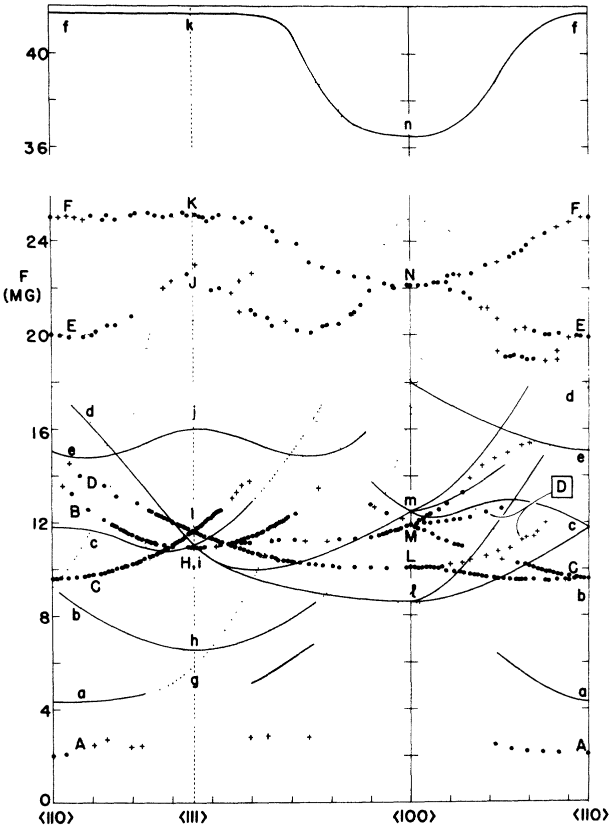

FIG. 1. A comparison of observed dHvA frequency data and expected frequency variations for the {110} and {100} planes. The most reliable experimental data (chiefly from rotations at constant field strength) are indicated by dark circles, and the crosses indicate data characterized by either low signal level (comparable with the periodogram noise level) or by large (>1%) scatter between successive field sweeps. The theoretical frequencies have been calculated graphically at symmetry directions from the Gupta-Loucks model, but the curves linking these values are schematic.

I at ⟨111⟩ can be related to the crossing of the predicted branches $ci\cdots$ and $di\cdots$. We also note that the observed branch $DI\cdots$ is found to split into two branches, DIL and DIM, a split which is in agreement with the topological requirements of the Gupta-Loucks model (curves dil and dim). Again, the observed minimum at H in branch $BH\cdots$ has a counterpart in the predicted minimum h, although here the numerical agreement is not as good; orbit h refers to the "hyperbolic" neck of the hole dumbbells (see Fig. 2), whose frequency should increase more rapidly than $1/\cos\theta$, where θ is the angle between the field and ⟨111⟩. This behavior is indeed found for the experimental points $BH\cdots$. We might add that, in the {100} plane, the experimental branches la-

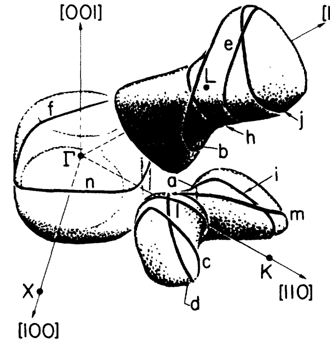

FIG. 2. The Gupta-Loucks model Fermi surface for thorium, showing various extremal orbits which are normal to the following symmetry directions: a,c, $[1\bar{1}0]$; b,e,f, [110]; d, [011]; h,j, [111]; i, $[\bar{1}10]$; l,m, [100]; n, [001]. The hole cube and the hole dumbbells are centered on the points Γ and L, respectively, while the electron lungs lie across the lines ΓK.

beled by the boxed D could not be followed all the way to their merging at ⟨110⟩, which would be required by our interpretation. The frequencies discussed so far refer to the relatively small orbits associated with the electron "lungs" and the central neck of the hole dumbbells; and we relate the higher frequencies $EJ\cdots$ and FKN to the larger orbits expected from the hole dumbbells and rounded cube, respectively.

The predicted and experimental frequencies are in fairly good numerical agreement for most of the orbits on the electron-"lung" surfaces (i.e., orbits c, d, i, l, and m). On the other hand, the experimental orbits on the hole dumbbells are larger than their calculated counterparts (b,h,e,j); but the extra hole volume implied by this increase in the size of the dumbbells appears to be offset by a decrease in the volume of the hole cube, a decrease which is a reflection of the fact that the observed orbits on the cube are smaller than the calculated ones (f,k,n). The many points of correspondence between the predictions of the Gupta-Loucks model and our dHvA results lend strong support to the essential correctness of the new model and hence to the basic premise of Gupta and Loucks that the band derived from the $5f$ level lies significantly above the Fermi energy.

Attempts are currently being made to extend the range of observation of the various frequency branches, and more detailed results will be reported in a future publication. We might add at this time that the observed cyclotron effective masses for the electron surfaces (m^*/m_0 ranging from 0.58 to 0.66) are larger than those predicted by the Gupta-Loucks band structure by a factor of roughly 1.4, which is similar to the mass enhancements described by Andersen and Mackintosh for various fcc transition metals.[9] A comparison of the observed and calculated masses for the hole surfaces would be premature at this stage because the matching between the experimental and predicted orbit sizes is less satisfactory for these surfaces.

We are indebted to Dr. D. T. Peterson for generously providing us with the refined thorium, to Dr. D. R. Stone for much helpful advice, and to Dr. R. P. Gupta and Dr. T. L. Louks for their close cooperation which has led to a satisfactory interpretation of our results.

---

*Work performed in the Ames Laboratory of the U. S. Atomic Energy Commission.

†National Aeronautics and Space Administration Trainee, 1966. Present address: Department of Physics, University of British Columbia, Vancouver 8, Canada.

‡Alfred P. Sloan Research Fellow. Present address: Department of Physics, University of British Columbia, Vancouver 8, Canada.

[1]A. C. Thorsen, A. S. Joseph, and L. E. Valby, Phys. Rev. 162, 574 (1967).

[2]D. T. Peterson, F. A. Schmidt, and J. D. Verhoeven, Trans. AIME 236, 1311 (1966).

[3]R. P. Gupta and T. L. Loucks, preceding Letter [Phys. Rev. Letters 22, 458 (1969)].

[4]D. T. Peterson and R. L. Skaggs, Trans. AIME 242, 922 (1968).

[5]W. R. Decker, D. L. Finnemore, and D. T. Peterson, Phys. Rev. Letters 18, 899 (1967).

[6]W. J. O'Sullivan and J. E. Schirber, Cryogen. 7, 118 (1967).

[7]R. W. Stark, Phys. Rev. 162, 589 (1967).

[8]R. F. Girvan, A. V. Gold, and R. A. Phillips, J. Phys. Chem. Solids 29, 1485 (1968).

[9]O. K. Andersen and A. R. Mackintosh, Solid State Commun. 6, 285 (1968).

FREE-CARRIER MAGNETO-OPTICAL EFFECTS IN FAR-INFRARED DIFFERENCE-FREQUENCY GENERATION IN SEMICONDUCTORS

N. Van Tran and C. K. N. Patel
Bell Telephone Laboratories, Holmdel, New Jersey
(Received 31 January 1969)

We report the first use of magnetoplasma effects for phase-matched nonlinear interactions in the far infrared.

The generation of tunable coherent radiation in the far-infrared (IR) spectrum (i.e., ~75-100 μ) is of considerable interest. Recently Zernike[1] and Yajima and Inoue[2] have reported far-IR generation by non–phase-matched difference-frequency mixing in bulk nonlinear media. The need for phase-matched operation in nonlinear mixing processes is important because it permits the use of long crystals for the far-IR generation. In this Letter we report the first use of a magnetoplasma effect for phase-matched difference-frequency generation in the 100-μ range by mixing the 9.6- and 10.6-μ CO_2 laser transitions in n-InSb. Phase matching is accomplished by the use of free-carrier contribution to the refractive index at ~100 μ. In particular perfect phase matching is obtained for difference frequencies in the 95- to 100-μ region by using a magnetic field for adjusting the propagation characteristics of the 100-μ radiation. For a given carrier concentration, the magnetic field at which phase matching occurs depends upon the difference frequency. Thus, the free-carrier magneto-optical effects offer a powerful technique for collinear phase-matched nonlinear interactions in the entire far-IR spectrum. We also report an estimate of the second-order nonlinear coefficient of InSb in the 100-μ range.

With powers P_{ω_1} and P_{ω_2} at infrared frequencies ω_1 and ω_2 incident on a nonlinear material of length l the difference frequency power output at $\omega_3=\omega_1-\omega_2$ is given by (in the near-field approximation)

$$P_{\omega_3(\mathrm{obs})}=\frac{32\pi^2\chi^2\omega_3^{\,2}}{3c^3n_1n_2n_3}\,\frac{P_{\omega_1}P_{\omega_2}T^3}{w^2}I, \tag{1}$$

where χ is the effective second-order nonlinearity (for InSb, $\chi=2d_{14}$); $n_{1,2,3}$ are the refractive indices at the three frequencies ω_1, ω_2, and ω_3, respectively; w^2 is the cross-sectional area of the incident beams at ω_1 and ω_2; T is power transmission coefficient for each surface of the sample; and I is the coherence factor (which also takes into account the losses in the nonlinear me-

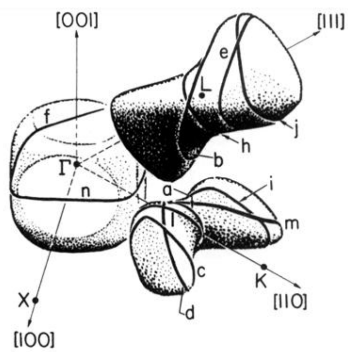

FIG. 2. The Gupta-Loucks model Fermi surface for thorium, showing various extremal orbits which are normal to the following symmetry directions: a, c, $[1\bar{1}0]$; b, e, f, [110]; d, [011]; h, j, [111]; i, $[\bar{1}10]$; l, m, [100]; n, [001]. The hole cube and the hole dumbbells are centered on the points Γ and L, respectively, while the electron lungs lie across the lines ΓK.